第29卷第2期 高能物理与核物理 Vol.29, No.2
2005年2月 HIGH ENERGY PHYSICS AND NUCLEAR PHYSICS Feb., 2005

Properties of the Gluon Recombination Functions*

ZHU Wei[1) SHEN Zhen-Qi
(Department of Physics, East China Normal University, Shanghai 200062, China)

Abstract The gluon recombination functions in the twist-4 QCD evolution equations are studied at the leading logarithmic approximation using both the covariant and noncovariant methods. We point out that the gluon recombination functions in the GLR-MQ evolution equation are unavailable. The methods avoiding the IR divergences are discussed, which can be used in the derivations of the evolution kernels and coefficient functions at higher twist level.

Key words gluon recombination, GLR-MQ equation, infrared(IR) divergence

1 Introduction

The QCD evolution equations in the leading order level predict strong rise of parton densities when the Bjorken variable $x_B = Q^2/2p.q$ decreases toward small values. This behavior violates unitarity. Therefore, various models are proposed to modify the twist-2 evolution kernels (i.e., the parton splitting functions). Gribov, Levin and Ryskin[1] first suggest a non-linear evolution equation, in which the evolution kernels (we call them the gluon recombination functions) are constructed by the fan diagrams. Later Mueller and Qiu[2] calculate the (real) gluon recombination functions at the double leading logarithmic approximation (DLLA) in a covariant perturbation framework. The GLR-MQ equation is broadly regarded as a key link from perturbation region to non-perturbation region. This equation was generalized to include the contributions from much higher order corrections in the Glauber-Mueller formula[3]. Following them, a similar evolution equation (we call it the modified DGLAP equation) is derived in a broader kinematic region (the leading logarithmic (Q^2) approximation-LLA(Q^2)) in Ref.[4]. Different from the GLR-MQ equation, the gluon recombination functions in this equation are calculated and summed in the (old-fashioned) time-ordered perturbation theory (TOPT).

In this paper we present the different results of the gluon recombination functions in the above-mentioned two evolution equations. The QCD evolution kernels are separated from the coefficient functions either in a covariant perturbation theory or in a parton model using TOPT. It is well known that these two approaches are completely equivalent. However, we find that the infrared (IR) singularities in the twist-4 Feynman diagrams impede us to safely extract the evolution kernels before these singularities are cancelled. This result leads to the fact that the gluon recombination functions in the GLR-MQ evolution equation are unavailable. For illustrating our idea in detail, in Sec. 2 we compare two approaches in the derivations of a splinting function in the twist-2 DGLAP equation[5]. Then we show two different derivations of the twist-4 recombination functions in Sec.3. In Sec. 4 we analyze the IR singularities in the recombination functions, which raise the questions in the derivations of the gluon recombination functions in the covariant theory. The discussions and conclusions are given in Sec. 5.

2 Twist-2 splitting functions

In this work we take the physical axial gauge and let the light-like vector n fix the gauge as $n.A = 0$, A being the gluon field, where $n^\mu \equiv \frac{1}{\sqrt{2}}(1, 0_\perp, -1)$ and $n^\mu \equiv \frac{1}{\sqrt{2}}(1,$

Received 16 August 2004
* Supported by NSFC(10075020, 90103013, 10475028)
1) E-mail: wzhu@phy.ecnu.edu.cn

$0_\perp$, 1). A natural derivation of the splitting function is given by TOPT in a special infinite momentum frame, i.e., the Bjorken frame, where the virtual photon has almost zero energy and zero longitudinal momentum. A Feynman propagator is decomposed into the forward and backward propagators in TOPT, where the propagating partons stay on-shell, respectively. One can find that the contributions of the backward components of the propagators in the cut diagram, for example in Fig.1(a) are suppressed[4]. Thus, the splitting function can be isolated in the equivalent particle approximation[6] as shown in Fig.1(b).

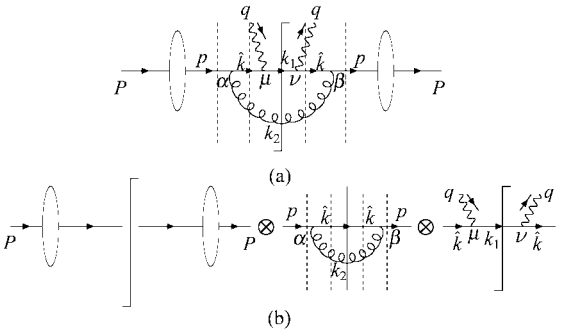

Fig.1. Graphical illustration of the isolation of a splitting function in the TOPT cut diagram. $\hat{k}$ is on-shell momentum and the dashed lines refer to the time order.

The contributions of Fig.1(a) to the twist-2 coefficient functions are

$$C^{\text{twist-2}}_{\text{TOPT}} = \int \frac{\mathrm{d}^3\boldsymbol{k}_2}{(2\pi)^3}\frac{1}{8E_{\hat{k}}E_{k2}}\left[\frac{1}{E_{\hat{k}}+E_{k2}-E_p}\right]^2 |\,M(\mathrm{q}\to\mathrm{qg})\,|^2 \times \frac{E_p}{E_{\hat{k}}}\bar{M}(\gamma^*\mathrm{q}\to\gamma^*\mathrm{q})\frac{x_{\mathrm{B}}}{Q^2}\delta(z-x_{\mathrm{B}}), \tag{1}$$

where we used

$$\mathrm{Tr}[\,\gamma_\mu \boldsymbol{k}_1\gamma_\nu \hat{\boldsymbol{k}}\gamma_\beta \boldsymbol{k}_2\gamma_\alpha \hat{\boldsymbol{k}}\,] = \mathrm{Tr}[\,\gamma_\mu \boldsymbol{k}_1\gamma_\nu \hat{\boldsymbol{k}}\,]\mathrm{Tr}[\,\gamma_\beta \boldsymbol{k}_2\gamma_\alpha \hat{\boldsymbol{k}}\,], \tag{2}$$

since the momentum $\hat{k}$ is on-shell. Now we can separately define a splitting function $P^{\mathrm{q}\to\mathrm{q}}_{\text{TOPT}}$(Fig.1(b)) as

$$\frac{\alpha_{\mathrm{s}}}{2\pi}\frac{\mathrm{d}k_{\mathrm{T}}^2}{k_{\mathrm{T}}^2}P^{\mathrm{q}\to\mathrm{q}}_{\text{TOPT}} = \frac{1}{8E_{\hat{k}}E_{k2}}\left[\frac{1}{E_{\hat{k}}+E_{k2}-E_p}\right]^2 |\,\bar{M}(\mathrm{q}\to\mathrm{q})\,|^2\frac{\mathrm{d}^3\boldsymbol{k}_2}{(2\pi)^3}, \tag{3}$$

i.e.,

$$P^{\mathrm{q}\to\mathrm{q}}_{\text{TOPT}} = \frac{4}{3}\left(\frac{1+z^2}{1-z}\right). \tag{4}$$

The same splitting function can be obtained in a covariant framework[7]. The related dominant Fynmann diagram for the coefficient function at the LLA (Q^2) is shown in Fig.2. For convenience, we take a collinear (infinite momentum) frame, in which the momenta of the initial parton and virtual photon are parameterized as

$$p = (p_z, \mathbf{0}, p_z) \equiv p_+\bar{n},$$

and

$$q \equiv q_+ n + q_- n \equiv -x_{\mathrm{B}}p_+ n + \frac{Q^2}{2x_{\mathrm{B}}p_+}n. \tag{5}$$

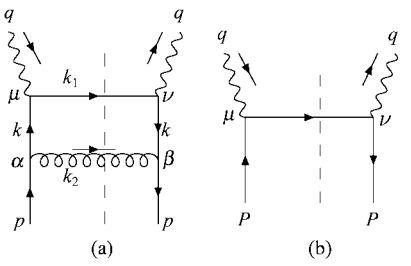

Fig.2. (a) A dominate covariant Feynman diagram for the twist-2 coefficient function at the LLA; (b) the bare virtual photon-quark vertex.

The contributions of the q→qg process in Fig.2 to the coefficient function are

$$C^{\text{twist-2}}_{\text{CVPT}} = \sum_i e_i^2\int\frac{\mathrm{d}^4k}{(2\pi)^3}\frac{\delta((k+q)^2)\delta((p-k)^2)}{k^4}M(\gamma^*\mathrm{q}\to\gamma^*\mathrm{q}), \tag{6}$$

where

$$\bar{M}(\gamma^*\mathrm{q}\to\gamma^*\mathrm{q}) = g^2\left\langle\frac{4}{3}\right\rangle_{\text{colour}}\frac{1}{4}\mathrm{Tr}[\,\gamma_\mu\gamma\cdot k_1\gamma_\nu\gamma\cdot k\gamma_\beta\gamma\cdot p\gamma_\alpha\gamma\cdot k\,]\Gamma_{\alpha\beta}(k_2)\,d^{\mu\nu}_\perp. \tag{7}$$

$\Gamma_{\alpha\beta}$ is an axial gauge gluon polarization

$$\Gamma_{\mu\nu}(k) = g_{\mu\nu} - \frac{k_\mu n_\nu + k_\nu n_\mu}{k\cdot n}. \tag{8}$$

In the calculations we use the Sudakov variables

$$k_\mu = bp_\mu + cq'_\mu + k_{\perp\mu}. \tag{9}$$

The result in the leading logarithmic region, where $k^2 \ll Q^2$ is

$$C^{\text{twist-2}}_{\text{CVPT}} = \sum_i e_i^2\frac{\alpha_{\mathrm{s}}}{2\pi}\int\frac{\mathrm{d}k_\perp^2}{k_\perp^2}\frac{4}{3}\frac{1+x_{\mathrm{B}}^2}{1-x_{\mathrm{B}}}. \tag{10}$$

The splitting function Eq.(4) can be directly obtained through dividing the coefficient function $C^{\text{twist-2}}_{\text{CVPT}}$ by the contributions of a bare photon-quark vertex (see Fig.2(b)), that is

$$P^{\mathrm{q}\to\mathrm{q}}_{\text{CVPT}} \equiv \frac{C^{\text{twist-2}}_{\text{CVPT}}}{C^{\mathrm{q}}_{\text{bare}}} = \frac{4}{3}\frac{1+z^2}{1-z}, \tag{11}$$

in which we have taken the assumption that

$$p_+ \gg q_-, \tag{12}$$

thus, one can define

$$k_+ = xP_+. \tag{13}$$

It is not surprising for the two approaches to have the above equivalence. In fact, the contributions of the backward components in two off-shell Feynman propagators in Fig.2 are suppressed under the conditions Eq.(12) and LLA (Q^2), although straightforward computations in covariant theory do not display this fact. To confirm this conclusion, we recalculate Eq.(10) but by removing the backward components in two Feynman propagators with the momentum k in Fig.2. We get the same result as Eq.(11).

3 Twist-4 recombination functions

The simplest way of the derivation of the recombination functions is TOPT, which was developed in Ref.[4]. In this method the recombination function is isolated from the twist-4 coefficient function using the equivalent approximation as shown in Fig.3 and it is generally written as

$$\alpha_s^2 R_{\mathrm{TOPT}}^{(p_1p_2\to p_3)} \mathrm{d}x_4 \frac{\mathrm{d}k_\perp^2}{k_\perp^4} = \frac{1}{16\pi^2} \frac{x_3x_4}{(x_1+x_2)^3} \times |M_{p_1p_2\to p_3p_4}|^2 \mathrm{d}x_4 \frac{\mathrm{d}k_\perp^2}{k_\perp^4}, \tag{14}$$

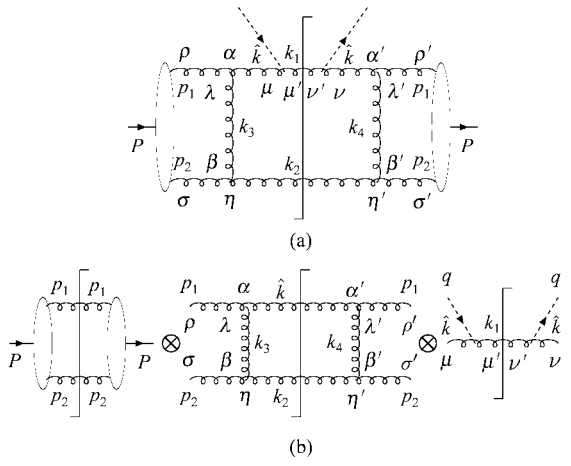

Fig.3. Graphical illustration of the isolation of a recombination function in the TOPT cut diagram. The dashed line is an effective "current" probing the gluonic matrix.

where $l_\perp^2 = p_x^2 + p_y^2$ and we use a current (the dashed lines) $-\frac{1}{4}F^{i\mu\nu}F^i_{\mu\nu}$ to probe the gluonic current[7].

The momenta of the initial and final partons are parameterized as

$$\begin{aligned} p_1 &= [x_1p, 0, 0, x_1p], p_2 = [x_2p, 0, 0, x_2p], \\ \hat{k} &= [x_3p + \frac{k_\perp^2}{2x_3p}, k_\perp, x_3p], \\ k_2 &= [x_4p + \frac{k_\perp^2}{2x_4p}, -k_\perp, x_4p], \\ k_3 &= [(x_4-x_2)p + \frac{k_\perp^2}{2x_4p}, -k_\perp, (x_4-x_2)p], \\ k_4 &= [(x_4-x_2)p + \frac{k_\perp^2}{2x_4p}, -k_\perp, (x_4-x_2)p]. \end{aligned} \tag{15}$$

For example, the recombination function for GG→G at t-channel is

$$R_{\mathrm{TOPT}}^{\mathrm{GG}\to\mathrm{G}} = \langle \frac{9}{8} \rangle_{\mathrm{color}} \frac{x_3x_4}{(x_1+x_2)^3} C_{\alpha\lambda\rho}C_{\beta\eta\sigma}C_{\alpha'\lambda'\rho'}C_{\beta'\eta'\sigma'}d_\perp^{\rho\rho'}d_\perp^{\sigma\sigma'} \times \frac{\Gamma_{\lambda\beta}(k_3)\Gamma_{\lambda'\beta'}(l_4)}{k_3^2k_4^2} \left(\delta^{lm} - \frac{\hat{k}^l\hat{k}^m}{|\hat{\boldsymbol{k}}|^2}\right)\left(\delta^{rs} - \frac{k_2^rk_2^s}{|\boldsymbol{k}_2|^2}\right), \tag{16}$$

where l, m, r, s are the space indices of $\alpha, \eta, \alpha', \eta'$ of k_3 and k_4, respectively; $C_{\alpha\lambda\rho}$ and $C_{\beta\eta\sigma}$ are the triple gluon vertex.

A set of recombination functions, where the contributions from all channels are summed up, is listed in Table 1.

Table 1.

$R_{\mathrm{TOPT}}^{\mathrm{GG}\to\mathrm{q\bar{q}}}$	$\frac{1}{48}\frac{(2y-x)^2(18y^2-21yx+14x^2)}{y^5}$
$R_{\mathrm{TOPT}}^{\mathrm{q\bar{q}}\to\mathrm{q\bar{q}}}$	$\frac{2}{9}\frac{(2y-x)^2}{y^3}$
$R_{\mathrm{TOPT}}^{\mathrm{qG}\to\mathrm{qG}}$	$\frac{1}{72}\frac{(2y-x)(16y^2+20yx+25x^2)}{y^4}$
$R_{\mathrm{TOPT}}^{\mathrm{q\bar{q}}\to\mathrm{GG}}$	$\frac{8}{27}\frac{(2y-x)(-10y^7+5yx+2x^2)}{y^3x}$
$R_{\mathrm{TOPT}}^{\mathrm{GG}\to\mathrm{GG}}$	$\frac{9}{64}\frac{(2y-x)(72y^4-48y^3x+140y^2x^2-116yx^3+29x^4)}{y^5x}$

Now let's return to discuss the recombination functions in CVPT. The gluon recombination functions in the GLR-MQ evolution equation are derived using CVPT at the double leading logarithmic approximation (DLLA), i.e., at the small x limit[2]. We use the same way to recompute the recombination functions but in the whole x region.

The coefficient function containing the gluon recombination function can be written as

$$C_{\mathrm{CVPT}}^{\mathrm{GG}\to\mathrm{G}} = \int \frac{\mathrm{d}^3k}{(2\pi)^3}\delta(k_1^2)\delta(k_2^2)|M_{\mathrm{GG}\to\mathrm{G}}|^2. \tag{17}$$

In the t-channel,

$$|M_{GG\to G}|^2 = g^4 < \frac{9}{8} >_{color} C^{\alpha\rho\lambda}C^{\beta\eta\rho}C^{\alpha'\rho'\lambda'}C^{\beta'\eta'\sigma'}v^{\mu\mu'}v^{\nu\nu'}d^{\rho\rho'}_{\perp}d^{\sigma\sigma'}_{\perp}$$
$$\frac{\Gamma_{\lambda\beta}(k_3)\Gamma_{\lambda'\beta'}(k_4)\Gamma_{\mu'\nu'}(k_1)\Gamma_{\mu\alpha}(k)\Gamma_{\nu\alpha'}(k)\Gamma_{\eta\eta'}(k_2)}{k^4k_3^2k_4^2}$$

where the current-gluon vertex v is

$$v^{\mu\nu} = k_\nu k_{1\mu} - g_{\mu\nu}k\cdot k_1, \tag{18}$$

and

$$\Gamma_{\lambda\beta}(k_3) = g_{\lambda\beta} - \frac{k_{3\lambda}n_\beta + k_{3\beta}n_\lambda}{k_3\cdot n} = d^{\lambda\beta}_{\perp} - 2\frac{k_3^-}{k_3^+}n^\lambda n^\beta. \tag{19}$$

The coefficient function of the contributions of a bare gluonic vertex is

$$C^G_{bare} = \frac{x_B}{2Q^2}. \tag{20}$$

Thus, the recombination function

$$R^{GG\to G}_{CVPT} \equiv \frac{C^{GG\to G}_{CVPT}}{C^G_{bare}}. \tag{21}$$

A set of complete recombination functions using the above-mentioned CVPT method is given in Table 2. A surprising result is that the recombination functions with the IR singularities in the CVPT method are inconsistent with that in the TOPT method. We shall detail it in the following section.

Table 2.

$R^{GG\to qq}_{CVPT}$	$\frac{1}{48}\frac{(2y-x)^2(18y^2-21yx+14x^2)}{y^5}$
$R^{qq\to qq}_{CVPT}$	$\frac{2}{27}\frac{(2y-x)^2(13y^2+6yx+3x^2)}{y^3(y-x)^2}$
$R^{qG\to qG}_{CVPT}$	$\frac{1}{36}\frac{(2y-x)(85y^4-93y^3x+106y^2x^2-93yx^3+31x^4)}{y^4(y-x)^2}$
$R^{qq\to GG}_{CVPT}$	$\frac{8}{27}\frac{(2y-x)(-10y^2+5yx+2x^2)}{y^3x}$
$R^{GG\to GG}_{CVPT}$	$\frac{9}{64}\frac{(2y-x)(144y^6-360y^5x+541y^4x^2-440y^3x^3+221y^2x^4-70yx^5+12x^6)}{y^5(y-x)^2x}$

4 IR safety in the recombination functions

At the first step, we point out that the IR singularities in R_{CVPT} originate from the gauge term in the gluon propagator $\Gamma^{\lambda\beta} = g^{\lambda\beta} - (k_3^\lambda n^\beta + k_3^\beta n^\lambda)/k_3\cdot n$, where $k_3\cdot n \sim y - x$ arris divergence if $y\to x$.

We decompose the propagator with the momentum k on the two gluon legs according to TOPT in Fig. 4. The on-shell propagating momenta are

$$k \to \hat{k}_F\left(zp_+\bar{n}, \frac{k_\perp^2}{2zp_+}n, k_\perp\right), \tag{22}$$

and

$$\hat{k}_B\left(\frac{k_\perp^2}{2zp_+}\bar{n}, zp_+\, n, k_\perp\right). \tag{23}$$

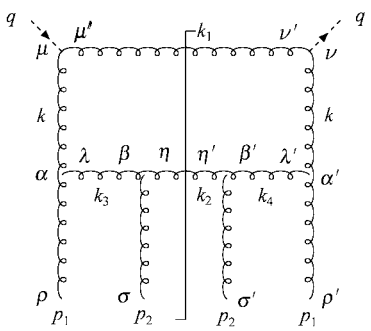

Fig. 4. A covariant Feynman diagram containing the gluon recombination function.

Where the sub-indices F and B refer to the forward and backward propagations, respectively. The dominant contributions in the LLA (Q^2) are from those terms with the highest power of $k_\perp^2$ in the numerator of the propagator. Obviously, term n^λ or $d^{\lambda\beta}_{\perp}$ in Eq. (19) can combine with $\hat{k}_B$ or $\hat{k}_F$ in Eqs. (22) and (23) through the quark-gluon or triple-gluon vertex, respectively. In consequence, the contributions from the forward and backward components coexist in the two propagators with the momentum k in these diagrams.

It is different from the recombination functions $R^{GG\to G}_{CVPT}$, the dominant numerator factor $\gamma\cdot n$ in $R^{GG\to G}_{TOPT}$ only chooses $\hat{k}_F$ in Eq. (22). Therefore, the contributions from the backward components are suppressed at the LLA (Q^2) and the equivalent particle approximation is available as in $R^{GG\to G}_{TOPT}$.

Such gauge singularities also exist in the derivation of the GLR-MQ equation[2], where an unusual $i\epsilon$ prescription is

used at limit $x \ll 1$ and the result is finite after taking the principal value. Obviously, the contributions from the backward components in the gluon propagators cannot be entirely excluded in this way. Thus, we can conclude that the recombination functions in the GLR-MQ equation are really a part of the twist-4 coefficient functions but not the evolution kernels since two legs in Fig.4 are off-shell.

Of cause, any physical results are IR safe. The IR divergences should be cancelled by summing up all related diagrams, including interference and virtual diagrams. After that one can isolate the recombination functions from the coefficient functions in the covariant framework. However, at the present moment we don't have an available way to calculate the virtual and interference diagrams. In the GLR-MQ equation such summations are evaluated using the Abramowsky-Gribove-Kancheli (AGK) cutting rule[8]. However, this application of the AGK cutting rule has been argued in Ref. [4]. Besides, the AGK cutting rules only change a relative weight in the contributions of the real diagrams and they cannot cancel any IR divergences.

Fortunately, the TOPT approach in the Bjorken frame provides an available method to derive the recombination functions. In fact, the recombination functions can be safely separated from the twist-4 coefficient functions in this way, since the backward components in two parton legs with the momentum k are suppressed. Thus, the equivalent parton approximation can be used. Furthermore, the contributions of the gauge singular terms disappear due to the absence of these backward components. To justify this conclusion, we use $d_\perp^{\mu\nu}$ to replace $\Gamma^{\mu\nu}$ in Eq.(16) and get the same results as Table 1.

Now let us look back to the CVPT method for the derivation of the recombination functions. According to the above-mentioned discussions, we use $d_\perp^{\lambda\beta}$ to replace $\Gamma_{\lambda\beta}$ in Eq.(19) As expected, one can get the same results as Table 1. From the above-mentioned discussions we can conclude that the forward propagators dominate the recombination functions.

5 Discussions and summary

An interesting question is why the IR singularities of the gluon propagator in the twist-2 coefficient function (Fig. 2 (a)) do not break the equivalent particle approximation. We note that this propagator through the dashed line is on-shell. Thus, Eq.(8) can be rewritten as

$$\hat{\Gamma}^{\alpha\beta} = d_\perp^{\alpha\beta} - \frac{k_\perp^2}{k_{2+}^2} n^\alpha n^\beta. \tag{24}$$

Now the dominant contributions to the LL A (Q^2) are only from the forward components and the equivalent particle approximation is applicable.

In summary, we show that the QCD evolution kernels are frame- and gauge-independent, however, the separation of these kernels from the coefficient functions depend on the frame and gauge. The IR singularities in the recombination functions inhibit us from safely isolating the recombination functions. This result leads to the fact that the gluon recombination functions in the GLR-MQ evolution equation are unavailable. The methods avoiding the IR divergences are discussed by using the TOPT.

References

1 Gribov L V, Levin E M, Ryskin M G. Phys. Rep., 1983, **100**: 1

2 Mueller A H, Qiu J. Nucl. Phys., 1986, **B268**: 427

3 Mueller A H. Nucl. Phys., 1990, **B335**: 115; Mueller A H. Nucl. Phys., 1994, **B415**: 373

4 ZHU W. Nucl. Phys., 1999, **B551**: 245

5 Altarelli G, Parisi G. Nucl. Phys., 1977, **B126**: 298

6 Kessler P. Nuovo Comento, 1966, **16**: 809; Baier V N, Fadin V S, Khoze V A. Nucl. Phys., 1973, **65**: 381; Chen M S, Zerwas P. Phys. Rev., 1975, **D12**: 187

7 Mueller A. Phys. Rep., 1981, **73**: 237

8 Abramovsky V A, Gribov J N, Kancheli O V. Sov. J. Nucl. Phys., 1973, **18**: 593

胶子重组函数的性质*

朱伟[1)] 沈祯祺
(华东师范大学理论物理研究所 上海 200062)

摘要 通过协变和非协变的方法研究了领头对数近似(LLA)下扭度为4的QCD演化方程中的胶子重组函数的性质.指出了GLR-MQ方程中的胶子重组函数并不适用.讨论了避免红外发散的方法,这种方法可以用于高扭度下演化核和系数函数的推导.

关键词 重组函数 QCD演化核 红外奇异

2004-08-16收稿
*国家自然科学基金(10075020,90103013,10475028)资助
1)E-mail:wzhu@phy.ecnu.edu.cn